Astronomy & Astrophysics

LETTER TO THE EDITOR

Why do protoplanetary disks appear not massive enough to form the known exoplanet population?

C. F. Manara[1],[*], A. Morbidelli[2], and T. Guillot[2]

[1] European Southern Observatory, Karl-Schwarzschild-Strasse 2, 85748 Garching bei München, Germany
 e-mail: cmanara@eso.org
[2] Laboratoire Lagrange, Université Côte d'Azur, Observatoire de la Côte d'Azur, CNRS, Boulevard de l'Observatoire, CS 34229, 06304 Nice Cedex 4, France

ABSTRACT

When and how planets form in protoplanetary disks is still a topic of discussion. Exoplanet detection surveys and protoplanetary disk surveys are now providing results that are leading to new insights. We collect the masses of confirmed exoplanets and compare their dependence on stellar mass with the same dependence for protoplanetary disk masses measured in ~1–3 Myr old star-forming regions. We recalculated the disk masses using the new estimates of their distances derived from *Gaia* DR2 parallaxes. We note that single and multiple exoplanetary systems form two different populations, probably pointing to a different formation mechanism for massive giant planets around very low-mass stars. While expecting that the mass in exoplanetary systems is much lower than the measured disk masses, we instead find that exoplanetary systems masses are comparable or higher than the most massive disks. This same result is found by converting the measured planet masses into heavy element content (core masses for the giant planets and full masses for the super-Earth systems) and by comparing this value with the disk dust masses. Unless disk dust masses are heavily underestimated, this is a big conundrum. An extremely efficient recycling of dust particles in the disk cannot solve this conundrum. This implies that either the cores of planets have formed very rapidly (<0.1–1 Myr) and a large amount of gas is expelled on the same timescales from the disk, or that disks are continuously replenished by fresh planet-forming material from the environment. These hypotheses can be tested by measuring disk masses in even younger targets and by better understanding if and how the disks are replenished by their surroundings.

Key words. planets and satellites: formation – protoplanetary disks – surveys

1. Introduction

At least 30% of stars have planets (e.g., Zhu et al. 2018) and, given current detection limits, it is plausible that planetary systems exist around every star. Similarly, in clusters younger than 2 Myr, ≳60–80% of stars possess protoplanetary disks (e.g., Fedele et al. 2010). Determining when these planets formed should be simple. It would require comparing the median mass of exoplanetary systems to the decrease in protoplanetary disk mass with age and determining the intersect. However, the lack of large samples of protoplanetary disk mass measurements and the incompleteness of exoplanet detection surveys have long hindered the task of constraining planet formation timescales. Furthermore, the fact that the millimeter emission from protoplanetary disks traces only the small dust mass (less than ~cm) and that total disk masses are still uncertain (e.g., Bergin & Williams 2017) makes the comparison more challenging.

Works based on surveys of protoplanetary disk masses carried out before the advent of the Atacama Large Millimeter/submillimeter Array (ALMA) and on initial results from radial velocity and transit planet detection surveys, indeed suggested that the mass of protoplanetary disks is usually lower than the mass of the detected giant planets. In particular,

Greaves & Rice (2010), Williams (2012), and Najita & Kenyon (2014) showed that only a tiny fraction of disks contain enough mass to explain the mass of the large number of observed gas giant planets in the standard core accretion model. They proposed that planet formation must have been underway by the time these disks were observed (~1–3 Myr). Similarly, Mulders et al. (2015, 2018) used the planet detections from the Kepler mission to show that the measured mass in disks around low-mass stars is typically smaller than the observed amount of heavy elements in the planetary systems around the same kinds of stars.

The time is now ripe to compare the masses of disks and planetary systems for a wide range of stellar types. Surveys of disks in several star-forming regions carried out with ALMA over the past few years, combined with optical to near-infrared spectroscopic surveys, are showing that the mass of the dust content of protoplanetary disks increases with stellar mass following a steeper than linear relation and decreases with time (e.g., Ansdell et al. 2016, 2017; Pascucci et al. 2016; Barenfeld et al. 2016). These results also show that disks around low-mass stars are less massive than the total mass in exoplanetary systems around similarly low-mass stars, for example TRAPPIST-1 (Pascucci et al. 2016; Testi et al. 2016). At the same time, surveys of exoplanets have now detected planets around stars with different stellar masses, and the dependences of the

---

[*] ESO Fellow.

planet properties on host star masses can be addressed (e.g., Mulders et al. 2018).

Here we perform for the first time a detailed comparison of the disk masses measured with ALMA in young star-forming regions with the current information on planetary systems masses, as well as core masses, to infer information on planet formation timescales and processes.

2. Sample and data

Exoplanet data are taken from exoplanet.eu (Schneider et al. 2011). From the catalog of 2018 July 10 we select only the confirmed planets. Since our analysis is based on the dependence of the stellar mass ($M_\star$) to the planet mass (M_{pl}), we only select targets for which these values are both available.

Starting from the catalog of confirmed exoplanets we construct our catalog of masses of exoplanetary systems by summing up the masses of individual planets in each system. These planetary masses are directly measured for ~80% of the exoplanetary systems. The reported masses represent a lower limit to the total mass in a system since planet detection surveys are still incomplete and a factor of $1/\sin(i)$ makes the actual masses larger most of the times. The masses of exoplanetary systems discussed here are still expected to be modified by future exoplanet detections. On the one hand, the masses of exoplanetary systems will increase when multiple planets in the known systems are detected. This will be a small or negligible effect, since only the lower mass planets are still unknown in a given exosystem. On the other hand, more sensitive exoplanet surveys will detect less massive planets, perhaps revealing the existence of other exoplanetary systems with overall lower total planet masses. These combined effects will increase the already wide (4 dex) spread of exoplanetary systems masses at any given stellar mass (see Fig. 1). However, the current data already allow us to draw reasonable preliminary conclusions on when and how planets form, as discussed in the following.

The measurements of protoplanetary disk masses (M_{disk}) are obtained from the surveys carried out with ALMA for disks in the ~1–3 Myr old Lupus and Chamaeleon I star-forming regions, the youngest regions extensively studied with ALMA to date (Ansdell et al. 2016; Pascucci et al. 2016). Disk dust masses are derived in these surveys by converting the millimeter continuum flux using a single value for the dust opacity and the disk temperature. Such measurements are thus only sensitive to grain sizes up to ~cm and are based on the emission from the outer regions of disks ($R > 10$ au; e.g., Bergin & Williams 2017). Disk total masses, inferred from gas emission lines, are still more uncertain (e.g., Miotello et al. 2017; Bergin & Williams 2017). For this reason, instead of using gas emission lines data, we estimate the total disk mass starting from the dust mass in disks and assuming a constant gas-to-dust ratio of 100. For these regions $M_\star$ is available for the vast majority of the disk-hosting stars from the spectroscopic surveys of Alcalá et al. (2014, 2017) in Lupus, and of Manara et al. (2016a, 2017) in Chamaeleon I. As discussed in Appendix A, we rescale the disk masses and stellar luminosity, and thus recalculate stellar masses, using the distances inferred from the newly delivered *Gaia* DR2 parallaxes (Gaia Collaboration 2016, 2018). The availability of accurately determined stellar masses is needed for our analysis. For this reason we cannot include the results of the survey in the ρ-Ophiucus region by Cox et al. (2017).

The dependence of both the exoplanetary systems, single exoplanets, and disk masses on the host star mass is shown in Fig. 1. As noted by Pascucci et al. (2016), among others, the
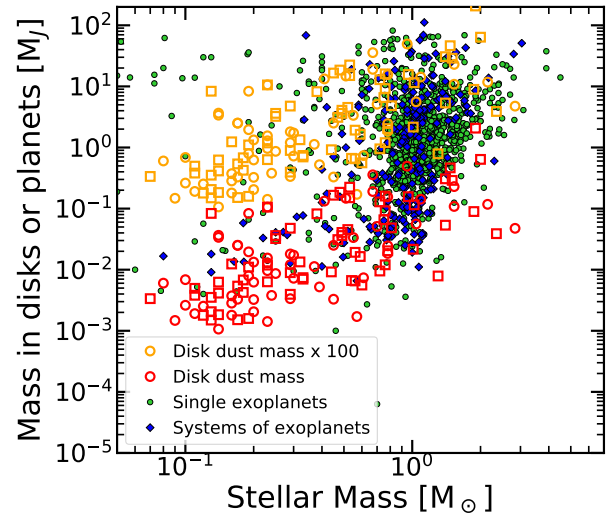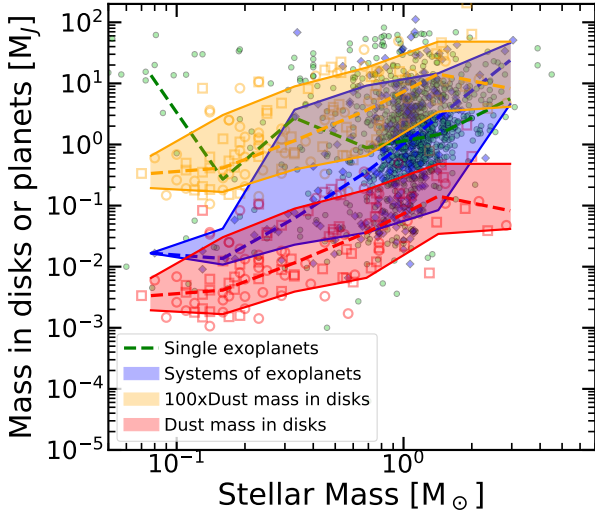

Fig. 1. Masses of single exoplanets, exoplanetary systems, and disk masses as a function of the mass of their host star. Empty squares are used for disks in the Chamaeleon I region, while empty circles for disks in the Lupus region.

dependence of disk masses on stellar masses for the targets in the Lupus and Chamaeleon I regions has a steeper than linear slope and the two distributions are indistinguishable, although the disks in the Lupus region are slightly more massive than those in the Chamaeleon I region (Ansdell et al. 2017). In the following, we consider the data from the two regions altogether. The main difference between the distribution of the masses of single exoplanet and systems of exoplanets is the population of very massive single exoplanets ($M_{pl} \gtrsim M_J$) around stars with $M_\star < 0.3\,M_\odot$, a region of the parameter space where no exoplanetary systems (i.e., only single planets) have been found to date. Since the mass ratio of these massive planets to their (small) host star is high (10^{-2} to ~1), it is plausible to infer that they may have been formed directly, as in binary stellar systems. In the following, we consider mainly the total masses in multiple exoplanetary systems for the comparison with the disk masses.

## 3. Comparison between disk and exosystem masses

When comparing the total mass in exosystems with the disk masses, we note that for low stellar masses ($M_\star \lesssim 0.3\,M_\odot$) the planetary system masses increase with stellar mass as the disk dust mass, although with a weak correlation. The median of the disk dust masses in this stellar mass range is a factor of ~0.2–0.3 of the exoplanetary system masses (Fig. 2), smaller than the expected >1 factor. It is possible that smaller planets are more difficult to detect, but since the upper envelope (90th percentile) of the distribution of disk dust masses is barely compatible with the median of the exosystem masses, the existence of smaller mass planets would not change the fact that there are planets more massive than the most massive disks. This means that exoplanetary system masses are usually higher, and in the best-case scenario comparable with disk dust masses. In this stellar mass regime planets have $M_{pl} \lesssim 10\,M_\oplus$, and they can be considered to be mainly rocky; instead, for higher stellar and planetary system masses, a wide spread of planet masses is present, with low-mass rocky planets as well as higher mass planets with gaseous envelopes detected. When comparing the planet masses with the total disk masses under the assumption of a constant

Fig. 2. Masses of single exoplanets, exoplanetary systems, and disk masses as a function of the mass of their host star, as in Fig. 1. The colored regions encompass the 10th and 90th percentiles of the distributions, while the dashed lines represent the median of the distributions, as labeled.

Fig. 3. Masses of the cores of single exoplanets and the sum of the cores in exoplanetary systems, as well as disk masses, as a function of the mass of their host star. The colored regions encompass the 10th and 90th percentiles of the distributions, while the dashed lines represent the median of the distributions, as labeled.

gas-to-dust ratio of 100, it is found that the median of the disk masses is higher than the median of the exoplanet masses by a factor of less than 10, while the 90th percentile of the two distributions are always comparable within a factor of 3. However, the assumption of a constant gas-to-dust ratio of 100 is uncertain.

We therefore perform a comparison of the disk dust masses with the core masses in planets and planetary systems. The main reasons for this choice is that the mass of planetary cores is mainly composed of the same heavy elements as the dusty component of disks, and that the disk dust masses are in general less uncertain than total disk masses. If the dust material in the disk has not yet grown to sizes larger than those probed by the millimeter flux of the disks, the disk dust material represents the material available to form planetary cores and rocky planets. The opposite possibility is considered in Sect. 4.1. For rocky planets, assumed here to be those with $M_{pl} < 10 M_{\oplus}$, we use their total mass as a tracer of the heavy element content. For more massive planets, instead, we convert the planet mass into core masses using the relation found by Thorngren et al. (2016) using a sample of 47 transiting planets. We calculate the total mass of heavy elements in exosystems by summing up the individual masses of rocky planets and cores of giant planets in each exosystem. The dependence of the total core planets masses on stellar mass is shown in Fig. 3 together with the disk dust masses. The median values of the disk dust masses are systematically ~0.2–0.3 times the heavy element content of planetary systems at all stellar masses <2 $M_{\odot}$. This confirms that the result obtained for disks and planets around low-mass stars is valid at all masses, and that the measured dust content in protoplanetary disks is smaller than the masses of the cores of exosystems. It is also worth noting that planetary systems are concentrated within a few au from the central star, whereas most of the disk mass is farther out. This makes the imbalance between planet masses and disk masses even more pronounced, as planet masses are much larger than the local disk masses. Planet migration and/or pebble accretion might help to alleviate this issue because both processes concentrate the solid mass from a large portion of the disk into its inner part. In the next section we address possible solutions to this conundrum.
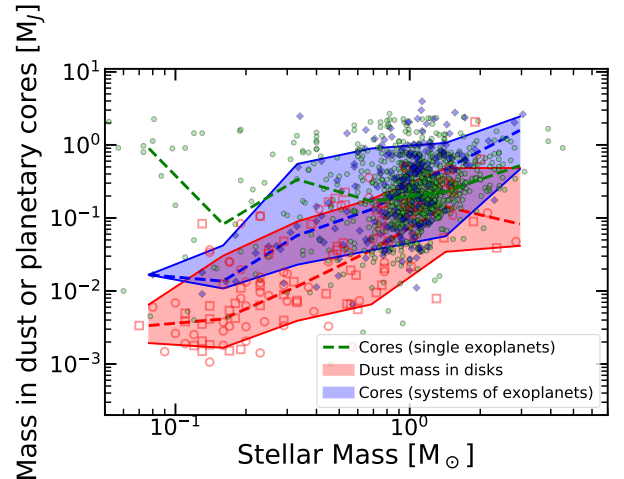
4. Discussion

The results shown in Sect. 3 pose a serious question of whether the protoplanetary disks have enough mass to form planets when they are ~1–3 Myr old, the age of the disks analyzed here. From the theoretical perspective, all models to explain the formation of planetesimals and planets are based on processes that are quite inefficient. In scenarios like pebble accretion (e.g., Johansen et al. 2007; Johansen & Lambrechts 2017; Ormel 2017), for example, only a small fraction of the pebble flux is captured by growing planets (see Guillot et al. 2014). If the total disk dust mass, calculated assuming a distribution of grain sizes, is a proxy of the amount of both small dust particles and pebbles, the disk dust mass is expected to be larger by at least one order of magnitude than the final mass in heavy elements in the planetary system. As we showed in Fig. 3, the heavy element content in exoplanetary systems can be as high as ~2–3 M_J for solar mass stars, and 0.02 M_J, about 6.4 $M_{\oplus}$, around brown dwarfs (e.g., the TRAPPIST-1 system, Gillon et al. 2017). In the solar system, summing up the mass in the terrestrial planets, in the cores of the giant planets, and in the progenitors of the Kuiper belt and Oort cloud, the total amount of heavy elements is about 130 $M_{\oplus}$, or 0.4 M_J (e.g., Guillot et al. 2014). On the contrary, the highest measured dust masses of protoplanetary disks at ~1–3 Myr are ~0.5–1 M_J around solar mass stars, and 0.01 M_J, ~3 $M_{\oplus}$, around brown dwarfs (see also discussion by Pascucci et al. 2016). These are also the masses of a tiny fraction of disks, whereas the bulk of the disk population has masses that are one order of magnitude smaller (see Fig. 3). This comparison shows that either planet accretion is more efficient than current models suggest or that other scenarios are needed.

A first naive possibility to explain this discrepancy is that the current surveys of exoplanets are biased towards high-mass planets, and the bulk of the population of exoplanets is instead much less massive than the one we observed. However, disk surveys are only targeting the disks that are still massive at ~1–3 Myr, and, for example, they do not include less massive disks which are optically thin in the near-infrared (Class III). These two biases should balance out.

Another possibility to explain the discrepancy is that disk dust masses are highly underestimated. It has been shown that

some dust mass can be confined into optically thick inner regions of disks (Tripathi et al. 2017; Ansdell et al. 2018) and that the opacity of disks and their temperature is still debatable (e.g., Andrews et al. 2013; Pascucci et al. 2016). It is also possible that a significant fraction of the dust content of disks has grown to cm sizes or more (e.g., Williams 2012; Najita & Kenyon 2014), and is thus not detected by millimeter observations. However, there are reasons to believe that disk masses are not underestimated by more than one order of magnitude. For example, significantly higher disk masses would make the measurements of faint CO emission lines (e.g., Miotello et al. 2017; Long et al. 2017) implying a gas-to-dust ratio much smaller than 100 even more difficult to explain, except in very old disks transitioning towards the debris phase. Furthermore, significantly underestimated disk dust masses would conflict with the observed general agreement of the measured disk masses and mass accretion rates with expectations from viscous evolution theory (e.g., Manara et al. 2016b; Rosotti et al. 2017; Lodato et al. 2017). As discussed by Pascucci et al. (2016), among others, this possibility is not enough to explain the apparent discrepancy between disk masses and planetary masses.

We do not believe that an efficient recycling of dust material in the disk is sufficient to explain the discrepancy. In such a scenario, the dust material that drifts inwards is then captured in disk winds originating in the innermost region of the disk ($R < 1$ au) and is redeposited in the outer disk ($R > 10$ au), where it will be able to again drift inwards. This scenario is commonly used to explain the observed population of calcium, aluminum-rich inclusions (CAI) and other aggregates present in bodies located throughout our solar system (e.g., Ciesla 2010; Desch et al. 2018). Within this scenario, the single dust particle has multiple possibilities to be accreted onto planetesimals or planets. This increases the overall efficiency of planet accretion (i.e., the probability that dust is ultimately incorporated into a planet). However, even in the best-case scenario where the efficiency grows to ~1, the total mass available for planet accretion would still be limited by $M_{disk,dust}$, which as we have seen is typically smaller than the observed total planet heavy element mass. Moreover, it is implausible that all the material in the disk is recycled. Indeed, the ratio of mass loss in winds to mass accreted onto the central star sets a generous upper limit to the fraction of particles that can be recycled. Since this ratio is usually measured to be <50%, and usually ~10% (e.g., Nisini et al. 2018), we consider that this scenario cannot explain the observed discrepancy between disk and planetary systems masses.

We propose in the following two possible explanations for the observations.

4.1. Early formation of planetary cores

One way to explain the observations is to postulate that the cores of planets are formed in the very first Myr of the protoplanetary disk evolution, or even in the embedded phase while the disk is still forming. The disks for which masses have been measured have ages >1 Myr, and a general trend of declining disk mass with ages older than 1 Myr has been observed (e.g., Barenfeld et al. 2016). Thus, it is possible that disks were massive enough to form the cores of planets at younger ages. This idea has been suggested by Greaves & Rice (2010), Williams (2012), and Najita & Kenyon (2014), among others. In this scenario, the vast majority of the material composing planets must already be in the form of planetesimals, for rocky planet formation, and of already-formed planetary cores. The latter condition is necessary as gas giant planets need to accrete gas from the gas-rich disk. Assuming a gas-to-dust ratio of 100, disks at ~1–3 Myr have just the right amount of gas mass to explain the population of gas giants (see Fig. 1). Thus, cores must already be in place at this age. Scenarios have been proposed to explain that pebble accretion can form planetesimals very early (<0.1 Myr) in disks, when these are massive and possibly gravitationally unstable (Booth & Clarke 2016). However, it is expected that the formation of planetary cores is highly inefficient, with ~350 $M_{\oplus}$ of pebbles needed to grow the core of Jupiter from half a lunar mass to 20 $M_{\oplus}$ (e.g., Morbidelli et al. 2016). Thus, such an inefficiency would imply that disks were initially ~10–100 times more massive than is observed at ages >1 Myr. This would also imply that the vast majority of disks were initially gravitationally unstable. One issue of this scenario is that, if early disks are ~10–100 times more massive than observed for disks older than 1 Myr, an extremely efficient gas-removal mechanism has to be found, consistent with the observations of Class 0 outflows (Frank et al. 2014).

This scenario is nevertheless in line with the recent result that the proto-core of Jupiter, with a mass of about 20 $M_{\oplus}$, formed very rapidly, within 1 Myr (Kruijer et al. 2017). Also, the rings observed in the disk around the still embedded <1 Myr old HL Tau protostar (ALMA Partnership 2015) may be carved by the presence of planets (e.g., Dipierro et al. 2015) suggesting, again, early planet formation. It should be noted that processes other than planet formation have also been invoked to explain the formation of these ringed structures in HL Tau (e.g., Lorén-Aguilar & Bate 2015).

4.2. Disks as conveyor belts

We explore here another possibility where the disks are similar to a conveyor belt that transports material from the environment to the central star. In this scenario, the disk is replenished with material from the surrounding interstellar medium either continuously or in various episodes (e.g., Throop & Bally 2008; Kuffmeier et al. 2017). This material, consisting of gas and small dust grains, is processed in the disk while drifting towards the central star. The material that is not processed in the disk is either accreted onto the central star or ejected through winds, and can even be partially recycled. This scenario is very similar to the one explored by Padoan et al. (2014) to explain the luminosity problem of embedded protostars, the dependence of the mass accretion rate onto the central star, and the presence of large grains in disks. Starting from the modeling of stellar cluster formation in turbulent molecular clouds, Padoan et al. (2014) have shown that the inferred infall rates onto the star-disk system, a sink particle in their simulation, are comparable to the mass accretion rates on the central star measured spectroscopically in young stellar objects (~10^{-12}–10^{-6} $M_{\odot}$ yr^{-1}, Manara et al. 2012), covering almost this whole range of values at any $M_{\star}$. A similarly vigorous accretion rate (~4×10^{-8} $M_{\odot}$ yr^{-1}) of material from the environment, in this case an envelope, onto the protoplanetary disk was measured by Semenov et al. (2005) for the AB Aur young stellar object, which has $M_{\star} \sim 2.4$ $M_{\odot}$. Assuming an accretion rate of 10^{-8} $M_{\odot}$ yr^{-1}, which is typical for all $M_{\star}$ in the simulations if such a process of accretion of material onto the disk from the environment is sustained for ~1 Myr after the time we are observing them, this would give to the disk 0.1 M_J of additional dust material (and 10 M_J of gas) to be used for planet formation. This value is comparable to the median of the measured disk dust masses for disks around stars with $M_{\star} \gtrsim 1$ $M_{\odot}$, similar to the AB Aur system. Disks around lower mass stars will have in general a lower accretion rate onto the disk, since in the

Bondy-Hoyle accretion scenario $\dot{M}_{acc} \propto M_{\star}^2$, but the scatter of the relation between the accretion rate from the environment onto the disk as a function of $M_{\star}$ has a large spread (Padoan et al. 2014), and it is thus possible that this process gives enough material to the disks to form planets. Simulations of face-on accretion of ISM material onto protoplanetary disks indeed show that the rate of material accreted onto the disk can even be as high as $10^{-6} M_{\odot}$ yr^{-1} depending on the density of the ISM material, on the relative velocity between the disk and the ISM, and on the disk sizes (Wijnen et al. 2016, 2017). However, it is still unclear how many star-disk systems are actually accreting material from the environment and whether this process is continuous or episodic.

Finally, it is worth noting that Scicluna et al. (2014) have even proved that disk-less stars going through over-densities of the local molecular cloud remnant are able to capture enough material to form a new disk around them, thus giving planet formation a second chance.

5. Conclusions

We collected the exoplanet and exoplanetary system masses and the masses of their host stars, and recalculated protoplanetary disk and disk-host star masses using the newly estimated distances based on *Gaia* parallaxes. We observe that single exoplanets around very low-mass stars can have masses almost as high as their host stars, whereas this is never observed in exoplanetary systems. This possibly points towards a different formation mechanism for these massive exoplanets around very low-mass stars. We have shown that current measurements of protoplanetary disk dust masses in ~1–3 Myr old regions are lower than or, at most, comparable to the amount of heavy element material in the exoplanetary systems discovered to date. Unless disk dust masses are underestimated by more than one order of magnitude, this result challenges the current theories of planet formation according to which planet formation should not be a very efficient process. We discuss two scenarios to explain this discrepancy: (i) an early formation of planetary cores at ages <0.1−1 Myr, when the disks may be more massive than those, much older, that are typically observed and (ii) the possibility that disks are replenished by fresh material from the environment during their lifetimes so that the total amount of material available for planet formation greatly exceeds that observed in the disk at any given time.

In order to confirm either of these hypotheses it is important to obtain measurements of disk dust masses and measurements of dust size distributions in disks in younger regions and in more embedded objects (Class 0/I), and to determine how many disks are replenished with material from the environment throughout their lifetimes.

References

Alcalá, J. M., Natta, A., Manara, C. F., et al. 2014, A&A, 561, A2
Alcalá, J. M., Manara, C. F., Natta, A., et al. 2017, A&A, 600, A20
ALMA Partnership, Brogan, C. L., Pérez, L. M. et al. 2015, ApJ, 808, L3
Andrews, S. M., Rosenfeld, K. A., Kraus, A. L., et al. 2013, ApJ, 771, 129
Ansdell, M., Williams, J. P., van der Marel, N., et al. 2016, ApJ, 828, 46
Ansdell, M., Williams, J. P., Manara, C. F., et al. 2017, AJ, 153, 240
Ansdell, M., Williams, J. P., Trapman, L., et al. 2018, ApJ, 859, 21
Baraffe, I., Homeier, D., Allard, F., & Chabrier, G. 2015, A&A, 577, A42
Barenfeld, S. A., Carpenter, J. M., Ricci, L., & Isella, A. 2016, ApJ, 827, 142
Bergin, E. A., & Williams, J. P. 2017, Astrophys. Space Sci. Lib., 445, 1
Booth, R. A., & Clarke, C. J. 2016, MNRAS, 458, 2676
Ciesla, F. J. 2010, Icarus, 208, 455
Cox, E. G., Harris, R. J., Looney, L. W., et al. 2017, ApJ, 851, 83
Desch, S. J., Kalyaan, A., & Alexander, C. M. O. 2018, ApJS, 238, 11
Dipierro, G., Price, D., Laibe, G., et al. 2015, MNRAS, 453, L73
Fedele, D., van den Ancker, M. E., Henning, T., Jayawardhana, R., & Oliveira, J. M. 2010, A&A, 510, A72
Frank, A., Ray, T. P., Cabrit, S., et al. 2014, Protostars and Planets VI, 451
Gaia Collaboration (Prusti, T., et al.) 2016, A&A, 595, A1
Gaia Collaboration (Brown, A. G. A., et al.) 2018, A&A, 616, A1
Gillon, M., Triaud, A. H. M. J., Demory, B.-O., et al. 2017, Nature, 542, 456
Greaves, J. S., & Rice, W. K. M. 2010, MNRAS, 407, 1981
Guillot, T., Ida, S., & Ormel, C. W. 2014, A&A, 572, A72
Johansen, A., Oishi, J. S., Mac Low, M.-M., et al. 2007, Nature, 448, 1022
Johansen, A., & Lambrechts, M. 2017, Ann. Rev. Earth Planet. Sci., 45, 359
Kruijer, T. S., Burkhardt, C., Budde, G., & Kleine, T. 2017, Proc. Nat. Acad. Sci., 114, 6712
Kuffmeier, M., Haugbølle, T., & Nordlund, Å. 2017, ApJ, 846, 7
Lodato, G., Scardoni, C. E., Manara, C. F., et al. 2017, MNRAS, 472, 4700
Long, F., Herczeg, G. J., Pascucci, I., et al. 2017, ApJ, 844, 99
Lorén-Aguilar, P., & Bate, M. R. 2015, MNRAS, 453, L78
Manara, C. F., Robberto, M., Da Rio, N., et al. 2012, ApJ, 755, 154
Manara, C. F., Fedele, D., Herczeg, G. J., et al. 2016a, A&A, 585, A136
Manara, C. F., Rosotti, G., Testi, L., et al. 2016b, A&A, 591, L3
Manara, C. F., Testi, L., Herczeg, G. J., et al. 2017, A&A, 604, A127
Miotello, A., van Dishoeck, E. F., Williams, J. P., et al. 2017, A&A, 599, A113
Morbidelli, A., Bitsch, B., Crida, A., et al. 2016, Icarus, 267, 368
Mulders, G. D. 2018, in Handbook of Exoplanets, eds. H. Deeg, & J. Belmonte (Cham: Springer)
Mulders, G. D., Pascucci, I., & Apai, D. 2015, ApJ, 814, 130
Najita, J. R., & Kenyon, S. J. 2014, MNRAS, 445, 3315
Nisini, B., Antoniucci, S., Alcalá, J. M., et al. 2018, A&A, 609, A87
Ormel, C. W. 2017, Astrophys. Space Sci. Lib., 445, 197
Padoan, P., Haugbølle, T., & Nordlund, Å. 2014, ApJ, 797, 32
Pascucci, I., Testi, L., Herczeg, G. J., et al. 2016, ApJ, 831, 125
Rosotti, G. P., Clarke, C. J., Manara, C. F., & Facchini, S. 2017, MNRAS, 468, 1631
Schneider, J., Dedieu, C., Le Sidaner, P., Savalle, R., & Zolotukhin, I. 2011, A&A, 532, A79
Scicluna, P., Rosotti, G., Dale, J. E., & Testi, L. 2014, A&A, 566, L3
Semenov, D., Pavlyuchenkov, Y., Schreyer, K., et al. 2005, ApJ, 621, 853
Siess, L., Dufour, E., & Forestini, M. 2000, A&A, 358, 593
Tazzari, M., Testi, L., Natta, A., et al. 2017, A&A, 606, A88
Testi, L., Natta, A., Scholz, A., et al. 2016, A&A, 593, A111
Thorngren, D. P., Fortney, J. J., Murray-Clay, R. A., & Lopez, E. D. 2016, ApJ, 831, 64
Throop, H. B., & Bally, J. 2008, AJ, 135, 2380
Tripathi, A., Andrews, S. M., Birnstiel, T., & Wilner, D. J. 2017, ApJ, 845, 44
Voirin, J., Manara, C. F., & Prusti, T. 2018, A&A, 610, A64
Wijnen, T. P. G., Pols, O. R., Pelupessy, F. I., & Portegies Zwart, S. 2016, A&A, 594, A30
Wijnen, T. P. G., Pols, O. R., Pelupessy, F. I., & Portegies Zwart, S. 2017, A&A, 602, A52
Williams, J. P. 2012, Meteorit. Planet. Sci., 47, 1915
Zhu, W., Petrovich, C., Wu, Y., Dong, S., & Xie, J. 2018, ApJ, 860, 101

Appendix A: Revised estimates of disk and stellar masses

In the light of the recent Data Release 2 (Gaia Collaboration 2018) of the *Gaia* mission (Gaia Collaboration 2016), we have revised the stellar masses and disk masses for all the targets in the samples of young stars with disks in the Lupus and Chamaeleon I star-forming regions. The data for the objects in these regions were initially analyzed assuming a distance of 150 pc or 200 pc for the targets in the Lupus region (Alcalá et al. 2017; Ansdell et al. 2016) and 160 pc for targets in the Chamaeleon I region (Manara et al. 2017; Pascucci et al. 2016). Here we queried the *Gaia* archive for all these targets to obtain the measured parallaxes and their uncertainties. We inverted the parallax measured in milliarcseconds to obtain the distance of the targets in parsec in the cases when the relative uncertainty on the parallax measurement was smaller than 10%. For the other targets with either more uncertain measurements of parallaxes or without a *Gaia* parallax measurement, we have assumed as a distance the inverted weighted mean of the parallaxes of all the objects in either the Lupus or Chamaeleon I samples. These median distances are 158.5 pc and 190 pc for the two regions, respectively. We note that the latter is well in line withe the estimate of Voirin et al. (2018) based on *Gaia* DR1 data. The distances used here are reported in Col. 3 of Tables A.1 and A.2.

The new estimates of stellar masses are obtained by rescaling the stellar luminosities from Alcalá et al. (2017) and Manara et al. (2017) to the new distances, and by comparing the new stellar luminosities and the effective temperatures of the stars with the evolutionary models by Baraffe et al. (2015), when possible, or Siess et al. (2000) for stellar masses higher
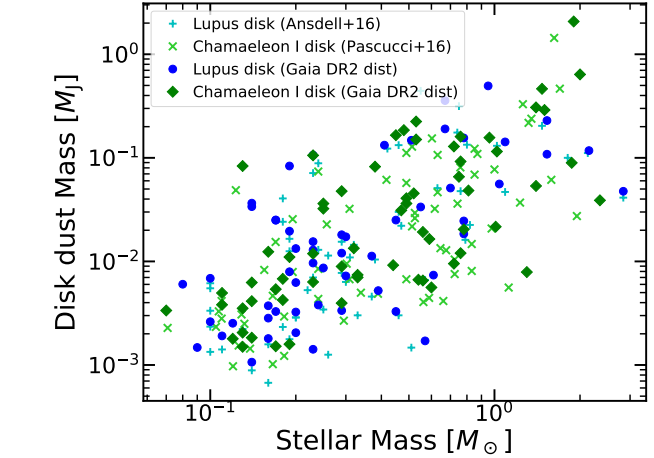
Fig. A.1. Disk mass vs stellar mass with new distances.

than 1.4 $M_\odot$. These newly determined stellar masses are reported in Col. 4 of Tables A.1 and A.2. Finally, the disk masses are obtained by rescaling the disk masses reported by Ansdell et al. (2016) and Pascucci et al. (2016) for the new distances, and are reported in Col. 5 of Tables A.1 and A.2.

As shown in Fig. A.1, the new distances do not drastically modify the overall distribution of the values of disk masses as a function of stellar masses with respect to previous works. Overall, we note that disk masses in the Chamaeleon I region are slightly higher than previously reported, while a slightly smaller spread is observed in the disk mass distribution for the disks in the Lupus region.

Table A.1. Stellar and disk masses for the objects in the Lupus star-forming region.

Name	Other names	Dist (pc)	$M_\star$ $M_\odot$	$M_{\mathrm{disk,dust}}$ $M_\oplus$
Sz65	Sz65	155.29	0.70	16.2437 ± 0.0806
Sz66	Sz66	157.34	0.29	3.8218 ± 0.0750
J15450887-3417333	SSTc2dJ154508.9-341734	154.96	0.14	11.6050 ± 0.1254
Sz68	Sz68	154.19	2.15	37.3405 ± 0.1142
Sz69	Sz69	154.55	0.20	4.2313 ± 0.0699
Sz71	Sz71	155.89	0.41	42.1459 ± 0.1600
Sz72	Sz72	155.89	0.37	3.5790 ± 0.0711
Sz73	Sz73	156.78	0.78	7.8125 ± 0.1413
Sz74	Sz74	158.50	0.30	5.4946 ± 0.0709
Sz81A	Sz81	159.86	0.19	2.5251 ± 0.0480
Sz82	Sz82	158.45	0.95	157.3413 ± 23.6012
Sz83	Sz83	159.57	0.67	113.5365 ± 0.1915
Sz84	Sz84	152.64	0.17	7.9432 ± 0.0973
Sz129	Sz129	161.68	0.78	49.4522 ± 0.1420
RYLup	RYLup	159.10	1.53	72.8398 ± 0.3067
J16000060-4221567	SSTc2dJ160000.6-422158	161.20	0.20	0.6514 ± 0.0516
J16000236-4222145	SSTc2dJ160002.4-422216	164.17	0.23	33.7391 ± 0.1774
J16002612-4153553	SSTc2dJ160026.1-415356	164.33	0.14	0.3385 ± 0.0536
Sz130	Sz130	160.27	0.39	1.6607 ± 0.0940
MYLup	MYLup	156.59	1.09	45.2837 ± 0.1946
Sz131	Sz131	160.31	0.30	2.3005 ± 0.0779
Sz133	Sz133	153.08	. . .	16.9009 ± 0.1885
Sz88A	Sz88	158.43	0.61	2.3438 ± 0.0786
J16070384-3911113	SSTc2dJ160703.9-391112	158.50	0.16	1.1860 ± 0.1443
Sz90	Sz90	160.40	0.78	5.8663 ± 0.1236
J16073773-3921388	Lup713	174.40	0.11	0.6068 ± 0.0572
Sz95	Sz95	158.17	0.29	1.0661 ± 0.0470
J16080017-3902595	Lup604s	159.89	0.12	0.8038 ± 0.0454
Sz96	Sz96	156.55	0.45	1.0444 ± 0.0717
J16081497-3857145	2MASSJ16081497-3857145	158.50	0.10	2.1832 ± 0.0787
Sz97	Sz97	157.75	0.24	1.2061 ± 0.0468
Sz98	Sz98	156.22	0.67	60.4867 ± 0.3620
Sz100	Sz100	136.94	0.14	10.7435 ± 0.1136
Sz103	Sz103	159.50	0.23	3.0664 ± 0.0744
J16083070-3828268	SSTc2dJ160830.7-382827	156.12	1.53	34.4472 ± 0.2851
Sz104	Sz104	165.46	0.16	0.9008 ± 0.0543
V856Sco	V856Sco	161.00	2.84	15.1102 ± 0.0758
Sz106	Sz106	161.67	0.57	0.5433 ± 0.0546
Sz108B	Sz108B	168.99	0.17	7.9851 ± 0.1015
J16084940-3905393	Par-Lup3-3	159.30	0.23	0.4506 ± 0.0450
V1192Sco	Par-Lup3-4	150.81	. . .	0.2162 ± 0.0451
Sz110	Sz110	159.51	0.23	4.0926 ± 0.0771
J16085324-3914401	2MASSJ16085324-3914401	167.71	0.29	5.7493 ± 0.0823
J16085373-3914367	2MASSJ16085373-3914367	158.50	0.10	0.8318 ± 0.0499
Sz111	Sz111	158.33	0.51	46.9712 ± 0.2566
J16085529-3848481	2MASSJ16085529-3848481	157.52	0.09	0.4691 ± 0.0466
Sz112	Sz112	160.27	0.17	1.0436 ± 0.0456
Sz113	Sz113	163.24	0.19	6.2207 ± 0.0751
J16090141-3925119	SSTc2d160901.4-392512	164.31	0.23	4.9349 ± 0.1918
Sz114	Sz114	162.25	0.19	26.5093 ± 0.1127
J16092697-3836269	SSTc2dJ160927.0-383628	159.35	0.20	1.0317 ± 0.0716
Sz117	Sz117	158.56	0.25	2.7494 ± 0.0473
Sz118	Sz118	163.90	1.04	17.7723 ± 0.2722
J16095628-3859518	Lup818s	156.93	0.08	1.9138 ± 0.0463
J16102955-3922144	SSTc2dJ161029.6-392215	163.23	0.20	1.9870 ± 0.0974
Sz123A	Sz123	158.50	0.55	10.6640 ± 0.1470
J16124373-3815031	SSTc2dJ161243.8-381503	159.81	0.45	7.9707 ± 0.1307
J16134410-3736462	SSTc2dJ161344.1-373646	160.00	0.16	0.5722 ± 0.0802

Notes. Original stellar masses are from Alcalá et al. (2014, 2017). Original disk masses are from Ansdell et al. (2016). The distances used to modify these values are from Gaia Collaboration (2018).

Table A.2. Stellar and disk masses for the objects in the Chamaeleon I star-forming region.

2MASS name	Other names	Dist (pc)	$M_\star$ $M_\odot$	$M_{\rm disk,dust}$ $M_\oplus$
2MASSJ10533978-7712338	...	191.81	0.33	2.2259 ± 1.7065
2MASSJ10555973-7724399	T3A	185.08	0.81	15.3631 ± 1.3908
2MASSJ10561638-7630530	ESOHalpha553	196.48	0.14	1.9879 ± 1.5696
2MASSJ10563044-7711393	T4	183.09	0.76	50.9436 ± 1.3219
2MASSJ10574219-7659356	T5	190.00	0.32	4.2586 ± 1.5444
2MASSJ10580597-7711501	...	186.57	0.11	1.2118 ± 1.4433
2MASSJ10581677-7717170	T6	189.84	1.47	147.4129 ± 1.4123
2MASSJ10590108-7722407	T7	185.21	0.76	29.3149 ± 1.3753
2MASSJ10590699-7701404	T8	187.48	2.00	203.0813 ± 1.3752
2MASSJ11004022-7619280	T10	191.54	0.23	33.5953 ± 1.4367
2MASSJ11022491-7733357	T11	176.26	1.50	92.0593 ± 1.2175
2MASSJ11025504-7721508	T12	182.24	0.19	0.5047 ± 1.4892
2MASSJ11040425-7639328	CHSM1715	192.31	0.18	1.3482 ± 1.5306
2MASSJ11040909-7627193	T14	191.78	0.96	49.8157 ± 1.4450
2MASSJ11044258-7741571	ISO52	193.15	0.23	2.0116 ± 1.5144
2MASSJ11045701-7715569	T16	194.46	0.29	1.2572 ± 2.0343
2MASSJ11062554-7633418	ESOHalpha559	209.30	0.13	26.5032 ± 1.7167
2MASSJ11064180-7635489	Hn5	195.28	0.17	0.4820 ± 1.7566
2MASSJ11065906-7718535	T23	190.34	0.25	11.5032 ± 1.4359
2MASSJ11065939-7530559	...	196.24	0.11	1.5752 ± 1.5836
2MASSJ11071206-7632232	T24	195.75	0.54	2.1143 ± 1.9855
2MASSJ11071860-7732516	ChaHalpha9	198.58	0.13	0.4760 ± 1.8295
2MASSJ11072074-7738073	T26	190.62	2.35	12.3622 ± 1.5004
2MASSJ11074245-7733593	ChaHalpha2	190.00	0.13	1.1201 ± 1.6764
2MASSJ11074366-7739411	T28	194.81	0.45	52.5996 ± 1.4903
2MASSJ11074656-7615174	CHSM10862	194.22	0.07	1.0675 ± 1.5858
2MASSJ11075730-7717262	CHXR30B	187.10	0.44	2.9235 ± 1.5474
2MASSJ11075792-7738449	T29	163.19	1.01	6.8730 ± 1.1208
2MASSJ11075809-7742413	T30	184.46	0.29	2.8416 ± 1.5023
2MASSJ11080148-7742288	T31	190.00	0.75	20.8577 ± 1.4490
2MASSJ11080297-7738425	ISO126	190.00	0.53	47.7823 ± 1.4183
2MASSJ11081509-7733531	T33A	190.00	1.40	97.5590 ± 1.4131
2MASSJ11083905-7716042	T35	188.36	0.78	6.4824 ± 1.5029
2MASSJ11085367-7521359	...	188.27	0.49	11.5165 ± 1.4639
2MASSJ11085464-7702129	T38	186.01	0.60	1.7817 ± 1.6551
2MASSJ11092266-7634320	C1-6	203.25	0.56	2.0788 ± 1.9762
2MASSJ11092379-7623207	T40	192.31	0.48	58.8523 ± 1.4513
2MASSJ11094621-7634463	Hn10E	195.04	0.33	2.3551 ± 1.7559
2MASSJ11094742-7726290	B43	192.96	0.53	71.2352 ± 1.4628
2MASSJ11095340-7634255	T42	201.96	0.72	40.9535 ± 1.6319
2MASSJ11095407-7629253	T43	190.00	0.52	14.4300 ± 1.4688
2MASSJ11095873-7737088	T45	191.29	0.47	9.8888 ± 1.4691
2MASSJ11100010-7634578	T44	192.08	1.90	658.7556 ± 1.4422
2MASSJ11100369-7633291	Hn11	201.01	0.59	5.2263 ± 1.7104
2MASSJ11100469-7635452	T45A	195.00	0.76	3.8183 ± 1.6431
2MASSJ11100704-7629376	T46	179.61	0.72	3.0229 ± 1.4048
2MASSJ11101141-7635292	ISO237	195.37	1.02	36.5996 ± 1.5194
2MASSJ11103801-7732399	CHXR47	190.00	1.30	2.5077 ± 1.6307
2MASSJ11104959-7717517	T47	185.16	0.38	26.1129 ± 1.3729
2MASSJ11105333-7634319	T48	194.68	0.29	15.1497 ± 1.5435
2MASSJ11105359-7725004	ISO256	195.77	0.16	3.9378 ± 1.5630
2MASSJ11105597-7645325	Hn13	140.23	0.12	0.5694 ± 0.8777
2MASSJ11111083-7641574	ESOHalpha569	190.00	. . .	25.6606 ± 1.4564
2MASSJ11113965-7620152	T49	190.51	0.25	10.2706 ± 1.4716
2MASSJ11114632-7620092	CHX18N	192.51	1.40	17.0085 ± 1.5003
2MASSJ11120351-7726009	ISO282	185.49	0.14	1.3134 ± 1.4191
2MASSJ11120984-7634366	T50	193.23	0.18	2.1573 ± 1.5650
2MASSJ11122772-7644223	T52	193.24	1.87	28.4416 ± 1.4909
2MASSJ11123092-7644241	T53	196.00	0.56	6.1133 ± 1.6065
2MASSJ11132446-7629227	Hn18	189.52	0.23	3.7763 ± 1.5473
2MASSJ11142454-7733062	Hn21W	188.95	0.19	3.5031 ± 1.4600
2MASSJ11160287-7624533	ESOHalpha574	190.00	. . .	6.0154 ± 1.6076
2MASSJ11173700-7704381	T56	188.38	0.49	12.9369 ± 1.4509
2MASSJ11183572-7935548	. . .	94.62	0.17	1.7129 ± 0.3583
2MASSJ11241186-7630425	. . .	184.75	0.13	0.6530 ± 1.4867
2MASSJ11432669-7804454	. . .	180.63	0.14	0.5826 ± 1.8409

Notes. Original stellar masses are from Manara et al. (2016a, 2017). Original disk masses are from Pascucci et al. (2016). The distances used to modify these values are from Gaia Collaboration (2018).